LncRNA FOXD3-AS1 Contributes to Glioblastoma Progression Via Sponging miR-3918 to Upregulate CCND1

Conggang HUANG[1, *], Ting SHAO[1,*], Faliang DUAN[1], Ruixue LI[2], Ming LUO[1], Qiaochun HUANG[1], Yuan WANG[1], Zhihua LUO[1]

[1]Wuhan No.1 Hospital, Department of Neurosurgery, Wuhan 430022, Hubei, China
[2]Wuhan No.6 Hospital, Intensive Care Unit, Wuhan 430014, Hubei, China

*These authors equally contributed to this work.

Corresponding author: Zhihua LUO ✉ zhihualuo5@163.com

ABSTRACT

AIM: To elucidate the pro-tumorigenic role of lncRNA FOXD3-AS1 in glioblastoma.

MATERIAL and METHODS: The expression of miR-3918, FOXD3-AS1, and CCND1 was measured in glioblastoma cells and tissues using reverse transcriptase quantitative PCR (RT-qPCR). The effect of FOXD3-AS1 silencing on the proliferation of glioblastoma cells was assessed in vitro using CCK-8 and colony formation assays and in vivo using xenograft mouse models. Additionally, the expression levels of the apoptosis-related proteins, Bcl-2 and Bax, were assessed using western blotting. Bioinformatic analysis and luciferase reporter assays assisted by RNA immunoprecipitation (RIP) and RNA pull-down experiments were conducted to validate the interactions among FOXD3-AS1, CCND1, and miR-3918.

RESULTS: FOXD3-AS1 and CCND1 were highly expressed in glioblastoma tissues and cells, whereas miR-3918 was poorly expressed. The expressions of FOXD3-AS1 and CCND1 were inversely associated with miR-3918 levels in glioblastoma tissues. FOXD3-AS1 silencing weakened the proliferative capacity and accelerated apoptosis of glioblastoma cells in vitro and hampered tumor growth in vivo. Mechanical investigations showed that FOXD3-AS1 knockdown increased miR-3918 expression and inhibited glioblastoma cell growth. Meanwhile, the miR-3918 inhibitor restored CCND1 expression and induced the opposite outcome.

CONCLUSION: FOXD3-AS1 facilitates the CCND1-driven progression of glioblastoma by serving as a competing endogenous RNA (ceRNA) for miR-3918. This suggests that FOXD3-AS1 may be a potential therapeutic target for the management of glioblastoma development.

KEYWORDS: Glioblastoma, Competing endogenous RNA (ceRNA), lncRNA FOXD3-AS1, Proliferation

■ INTRODUCTION

Glioblastoma, also known as glioblastoma multiforme (GBM), is a highly aggressive intracranial tumor that accounts for approximately 50% of primary malignant brain tumors (19). Although glioblastoma management has advanced significantly, the clinical outcome of individuals suffering from this disorder has been poor, with a median survival time of less than one year (7). Many genetic and environmental factors have been shown to play important roles in gliomagenesis (9). Therefore, a better understanding of the molecular mechanisms underlying glioblastoma malignancy is required.

Recently, transcriptome investigations have revealed that non-coding RNA (ncRNAs) constitute approximately 99% of the human genome. Long noncoding RNAs (lncRNAs) are noncoding transcripts ≥200 nt in length. They function as epigenetic regulators and regulate various biological regulatory activities (15). Increasing evidence has confirmed that mu-

Conggang HUANG (ID) : 0000-0001-8824-0129
Ting SHAO (ID) : 0000-0002-8263-7106
Faliang DUAN (ID) : 0000-0002-9510-1095

Ruixue LI (ID) : 0000-0002-0166-0874
Ming LUO (ID) : 0000-0001-9011-7234
Qiaochun HUANG (ID) : 0000-0002-3922-7662

Yuan WANG (ID) : 0000-0003-1655-0157
Zhihua LUO (ID) : 0000-0002-8205-4445

tation and dysregulation of lncRNAs are some of the major etiological factors for various disorders, including tumors (1). Emerging lncRNAs have been reported as putative players in glioblastoma genesis and progression. For instance, Zhou *et al.* reported that lncRNA AC005013.5, AC073115.6, UBE2R2-AS1, ENTPD1-AS1, RP11-89C21.2, and XLOC_004803 are inferior prognostic signatures in glioblastoma multiforme cohorts (24). Moreover, the oncogenic lncRNA SNHG12 activates the MAPK/ERK pathway to regulate temozolomide chemoresistance in glioblastoma (13). In addition, targeting lncRNA MALAT1 in intracranial xenograft models of glioblastoma could increase the sensitivity of cancer cells to chemotherapeutic drugs (18). Regarding lncRNA FOXD3-AS1, its pro-tumoral role has been demonstrated in different cancers. For example, FOXD3-AS1 acts as a critical regulator of oncogenic TGF-β1/Smads and promotes thyroid cancer progression (5). Furthermore, FOXD3-AS1 acts as a competing endogenous RNA (ceRNA) for various microRNAs (miRNAs), such as miR-150 (8) in non-small cell lung cancer (NSCLC) and miR-325 (4) in cutaneous malignant melanoma, to enhance the expression of the miRNAs' downstream genes. This results in the promotion of tumor cell proliferation and invasion. However, its specific function and mechanism of action in glioblastoma remain unclear.

Here, we focused on FOXD3-AS1's role in glioblastoma *in vivo* and *in vitro*. Analyzing the molecular function of FOXD3-AS1 has revealed its ceRNA activity, in which it regulates glioblastoma cell progression through a novel miRNA/mRNA axis. Our results suggest a potential mechanism for FOXD3-AS1-mediated uncontrolled proliferation of glioblastoma cells. This study also contributes to new insights into glioblastoma management.

■ MATERIAL and METHODS

Clinical Specimens

Seventeen sets of glioblastoma tumors and matched normal brain tissues were obtained from individuals with glioblastoma. The patients were enrolled between 2018 and 2020 at Wuhan No. 1 Hospital. All the tissues were re-evaluated by two independent pathologists. All specimens were maintained at −80 °C for detecting the indicated genes via RT-qPCR. Ethics approval was provided by the Ethics Committee of Wuhan No. 1 Hospital. All the enrolled patients signed a written consent form.

Cell Culture

Normal human astrocytes (NHA), which served as control cells, were purchased from Lonza, Basel, Switzerland. The glioma cell lines U251, A172, and SHG-144 were obtained from the American Type Culture Collection (ATCC). The glioma cell lines were cultured in Dulbecco's modified Eagle's medium (DMEM; Gibco, USA) containing 10% fetal bovine serum (FBS; Thermo Fisher, USA). NHAs were cultured in astrocyte growth media (Lonza, Basel, Switzerland) supplemented with 5% FBS. The cultures were maintained in 5% CO_2 at 37 °C.

Cell Transfection

Short hairpin RNAs (shRNAs) that target FOXD3-AS1 (sh-lnc) and its negative control (sh-NC), si-FOXD3-AS1 (si-lnc), si-CCND1 and their si-NCs, and miR-3918 inhibitor/mimic and their NCs were sourced from GeneCopoeia, USA. Lipofectamine™ 3000 Reagent (Thermo Fisher, USA) was used for cell transfection. For FOXD3-AS1 silencing, lentiviral shRNA transduction particles carrying FOXD3-AS1 shRNAs (sh-lnc) and sh-NCs were used to infect U251 cells at 80% confluency for 48 h. The methodology was based on the product protocol. Then, 2 μg/mL puromycin was added for 24 h for selecting the cells. Cells that exhibited resistance to puromycin were gathered and analyzed via RT-qPCR. For other transfections, the indicated duplexes were introduced into U251 and A172 cells at 80% confluence for 48 h. Finally, RT-qPCR was conducted to gauge their transfection efficiencies.

Cell Proliferation Assays

Cell Counting Kit-8 (CCK-8) and colony formation experiments were performed to assess the proliferative capacity of the glioblastoma cell lines. For the CCK-8 assay, 5×10^4 A172 or U251 cells per well were cultured in 96-well plates. After 24, 48, 72, and 96 h of cultivation, the cells were exposed to 10 μL CCK-8 reagent (Abcam, USA) for 1 h. Finally, the absorbance readings were obtained at a wavelength of 450 nm for each well using a Multiskan Spectrum (Thermo Fisher, USA).

For colony formation experiments, 500 A172 and U251 cells were inoculated into each well of a 6-well culture plate. The cells were maintained for 2 weeks, followed by fixation and staining with 4% paraformaldehyde and methyl violet (Beyotime, China). Finally, the number of colonies was counted using an inverted microscope (Nikon, Tokyo, Japan).

RT-qPCR

Total RNAs was isolated from clinical tissues or cells using TRIzol reagent (Legend Biotech, China). Reverse transcription of cDNA was carried out with the aid of a TaqMan® MicroRNA Reverse Transcription Kit (Thermo Fisher, USA) and a PrimeScriptTM RT Reagent Kit with gDNA Eraser (Takara, Japan). A FastStart DNA SYBR Green I Kit (Roche, Switzerland) was used for real-time PCR, which was performed in an Applied Biosystems (ABI) 7500 Sequence Detection System (Thermo Fisher, USA). The relative expression levels of FOXD3-AS1, miR-3918, and CCND1 were determined using the $2^{-\Delta\Delta Ct}$ approach (12), with U6 or GAPDH as the housekeeping genes. All primers used are listed in Table I.

Western Blotting

Whole-cell lysates containing proteins were acquired using radioimmunoprecipitation assay (RIPA) buffer (Amylet Scientific, China). A Bio-radDC Protein Assay Kit (Bio-Rad, China) was used to quantify the protein concentration. A 10% SDS-PAGE gel was used for the separation of proteins before transferring them onto polyvinylidene fluoride membranes. Subsequently, 5% non-fat dry milk was added to the membranes for sealing. The membranes were incubated at room temperature before exposure to anti-Bax (K106624P, 1:1000), anti-Bcl-2 (K003505P, 1:1000), anti-GAPDH (K200057M, 1:1000), and

Table I: The Sequences of the Primers in This Study

Primer	Sequences
FOXD3-AS1	Forward: 5′-GAATAGTTGCCGAGAGAAA-3′
	Reverse: 5′-GACAGACAGGGATTGGGTT-3′
CCND1	Forward: 5′-GTCTGCGAGGAACAGAAGTG-3′
	Reverse: 5′-TTAGAGGCCACGAACATGC-3′
WNT5A	Forward: 5′-TCGACTATGGCTACCGCTTT-3′
	Reverse: 5′-CACTCTCGTAGGAGCCCTT-3′
EGFR	Forward: 5′-TCCCTCAGCCACCCATATGTAC-3′
	Reverse: 5′-GTCTCGGGCCATTTTGGAGAATCC-3′
STAT3	Forward: 5′-ACTTTCACTTGGGTGGAGAAGGACAT-3′
	Reverse: 5′-CTGCTGCTTTGTGTATGGTTCCA-3′
GAPDH	Forward: 5'-AGAAGGCTGGGGCTCATTTG-3'
	Reverse: 5'-AGGGGCCATCCACAGTCTTC-3'
U6	Forward: 5'-TGCGGGTGCTCGCTTCGGCAGC-3'
	Reverse: 5'-CCAGTGCAGGGTCCGAGGT-3'

anti-CCND1 (K006377P, 1:1000) antibodies at 4°C. All antibodies were acquired from Solarbio (Beijing, China). The following day, the corresponding horseradish peroxidase-conjugated (HRP) secondary antibodies (SA205, 1:1000, Solarbio, China; A32723, 1:1000, Thermo Fisher, USA) were added. The membranes were maintained at 37 °C for 1 h to detect the bands. Finally, the signals were visualized using Western Lightning Plus-ECL, Enhanced Chemiluminescence Substrate (PerkinElmer, USA). Protein quantification was conducted using the ImageJ software.

Luciferase reporter assay

Wild-type (WT) fragments of 3'-UTR FOXD3-AS1 and 3'-UTR CCND1 carrying miR-3918 putative binding sites and their corresponding partially or completely mutated (MUT) segments were subcloned into a luciferase reporter plasmid. The following vectors were used: pMIR-FOXD3-AS1-WT, pMIR-FOXD3-AS1-MUT, pMIR-CCND1-WT, pMIR-CCND1-MUT1, pMIR-CCND1-MUT2, and pMIR-CCND1-Co-MUT. Luciferase reporter constructs, along with either an miR-3918 mimic or NC, were introduced into the U251 and A172 cells to detect luciferase activity. The next day, Promega's luciferase reporter system was used to measure the luciferase activity.

RNA pull-down assay

MiR-3918 with a 3'-biotin label (bio-miR-3918) and its negative control (bio-NC) were obtained from GemaPharma (Shanghai, China). The A172 and U251 cells were seeded into a 10-cm tissue culture plate and transfected with either bio-miR-3918 or bio-NC with the aid of a RNAiMAX (Invitrogen, USA). The cell lysate was prepared 48 h post transfection. Subsequently, the supernatant was obtained after centrifugation and maintained with Streptavidin-Dyna beads at 4 °C for 2 h in a rotator. After repeatedly washing the beads with lysis buffer, the WNT5A, EGFR, STAT3, and CCND1 genes were quantified by RT-qPCR.

RNA immunoprecipitation (RIP) assay

An RIP Kit (Millipore Sigma, USA) was used to validate the interaction between FOXD3-AS1 and miR-3918. In brief, ~80% confluent A172 and U251 cells (2 million cells/tube) were collected and exposed to 200 μL of a mild or strong lysis buffer for 30 s. After centrifugation at 16,000 × g and 4°C for 10 min, the supernatant was prepared and continuously incubated at 4 °C with pre-prepared Anti-AGO2 or Anti-IgG beads. Thirty minutes later, the magnetic stand was collected and washed with lysis buffer before RT-qPCR analysis.

Subcellular fractionation

A FractionPREP™ Cell Fractionation Kit (Biovision, USA) was used to separate the nuclear and cytoplasmic fractions according to the manufacturer's instructions. RT-qPCR was conducted to evaluate the FOXD3-AS1 levels in both fractions. GAPDH or U6 was used as the housekeeping gene.

Xenografts in mice

Ten female pathogen-free, 6-week-old C57BL/6 mice weighing 20–25 g were obtained from the Experimental Animal Center of Wuhan University (Wuhan, China). The mice were randomly divided into two groups, maintained in ventilated cages, and subjected to a 12 h light/12 h dark cycle. The procedures performed in this animal study were approved by the Animal Ethics Committee of the Wuhan No. 1 Hospital (Wuhan, China). After 7 days of adaptation, 1×10^5 A172 cells (100 μL) stably transfected with either sh-NC or sh-lnc were administered subcutaneously into the mice to construct a human xenograft tumor model. After five weeks, euthanasia by CO_2-inhalation was carried out among the mice before their tumors were excised and weighed.

Statistical Analysis

GraphPad Prism 9.0 (GraphPad Prism Software, USA) was utilized to analyze data. The figures were in the format of mean ± standard deviation (SD). *P*-value of comparisons between experimental groups were calculated using Student's *t*-test and one-way ANOVA with Tukey's post-hoc test for comparison of multiple groups. Pearson's correlation was used in determining the associations of the genes. The results are statistically significant if $p < 0.05$.

■ **RESULTS**

FOXD3-AS1 silencing displays inhibitory effect on the growth of glioblastoma *in vivo* and *in vitro*

The GEPIA database indicated FOXD3-AS1 was more upregulated in glioblastoma samples than in controls (Figure 1). To evaluate FOXD3-AS1's biofunction in glioblastoma, we first assessed its levels in glioblastoma cells and tissue samples.

As indicated by the RT-qPCR results, the amplification of FOXD3-AS1 was observed in glioblastoma tissues (Figure 2A). High expression was also observed in glioblastoma cell lines (Figure 2B). This was particularly evident among the A172 and U251 cells, as they exhibited an almost 8-fold increase in FOXD3-AS1 levels, unlike the NHA cells. To further dissect its mechanism in glioblastoma progression, we conducted cell fractionation to determine the location of FOXD3-AS1 in A172 and U251 cells. Remarkably, FOXD3-AS1 was enriched in the cytoplasmic fraction (Figure 2C). This suggests that FOXD3-AS1 has ceRNA activity in glioblastoma cells. Cell function experiments were conducted to assess the effects of FOXD3-AS1 silencing on glioblastoma cell proliferation. FOXD3-AS1 was knocked down in A172 and U251 cells. The resulting cells were single-cell-sorted, and successful FOXD3-AS1 silencing was verified by RT-qPCR (Figure 2D). The results of the CCK-8 assay showed that FOXD3-AS1-knockdown cells displayed an obvious reduction in cell proliferation (Figure 2E). The clone formation assay further demonstrated a reduced proliferation phenotype in A172 and U251 cells with silenced FOXD3-AS1 (Figure 2F). As apoptosis is associated with cell proliferation, we further investigated Bcl-2 and Bax, which are some of the proteins involved in apoptosis. As demonstrated by western

blotting (Figure 2G), FOXD3-AS1 silencing resulted in an increase in Bax and a reduction in Bcl-2 levels, suggesting enhanced apoptosis. Afterwards, we performed *in vivo* assays to assess the functional influence of FOXD3-AS1 silencing on glioblastoma tumorigenesis. Injecting A172 cells transfected with sh-lnc into C57BL/6 mice reduced tumor volume in 5 weeks, as alongwith a 70% reduction in tumor weight, unlike those carrying sh-NC (Figure 2H). Overall, the results from *in vitro* and *in vivo* experiments suggest that FOXD3-AS1 promotes glioblastoma tumorigenesis and development.

### FOXD3-AS1 is a negative upstream regulator of miR-3918

As FOXD3-AS1 was abundant within the cytoplasm of A172 and U251 cells, we analyzed its ceRNA activity in glioblastoma. According to the starBase prediction, FOXD3-AS1 and miR-3918 shared binding sites (Figure 3A). Luciferase reporter assays were performed to test this hypothesis. The results of luciferase assays demonstrated that miR-3918 amplification resulted in a significant impairment in FOXD3-AS1-WT-induced luciferase activity in A172 and U251 cells. However, it exerted no effect on FOXD3-AS1-MUT-induced luciferase activity (Figure 3B). AGO2 pull-down analysis was conducted to confirm the interaction between miR-3918 and FOXD3-AS1. The results showed that the AGO2 precipitate was highly enriched with miR-3918 and FOXD3-AS1 (Figure 3C). Interestingly, we also observed low levels of miR-3918 in glioblastoma cells and tissue samples (Figures 3D and 3E). This interaction was further confirmed by Pearson's test, which revealed a negative correlation between them (Figure 3F). These results suggest that FOXD3-AS1 targets miR-3918.

FOXD3-AS1 interacts with miR-3918 to carry out its pro-proliferative function in glioblastoma cells

Assessment of proliferation phenotypes in glioblastoma cells was conducted to verify whether their interaction influences cell function. We first transfected si-lnc, si-NC, inhibitor-NC, miR-3918 inhibitor, or si-lnc+miR-3918 inhibitor into the A172 and U251 cells. As indicated by the RT-qPCR results, miR-3918 expression increased upon si-lnc transfection. However, this outcome was almost eliminated by transfection with the miR-3918 inhibitor (Figure 4A). As indicated by CCK-8 and colony formation results, the miR-3918 inhibitor increased the proliferation of glioblastoma cells, but this phenomenon was nullified by silencing FOXD3-AS1 (Figure 4B and 4C). In addition, FOXD3-AS1 silencing almost reversed the upregulation of Bcl-2 and downregulation of Bax caused by the absence of the miR-3918 inhibitor (Figure 4D). Collectively, FOXD3-AS exerted its tumor-promoting function in glioblastoma by serving as miR-3918's ceRNA.

CCND1 is a direct downstream target of miR-3918

It has been established that mRNAs are the effectors of lncRNA ceRNA activity. Therefore, we explored the mRNA interacting with theFOXD3-AS1/miR-3918 axis. TargetScan and starBase were used to identify downstream targets of miR-3918. GSE10429, an mRNA microarray from GEO DataSets, was also utilized to survey the upregulated genes in GBM, with an adj. $P<0.05$ and logFC>2. The results showed that 107 common genes from TargetScan, starBase, and GSE10429 overlapped
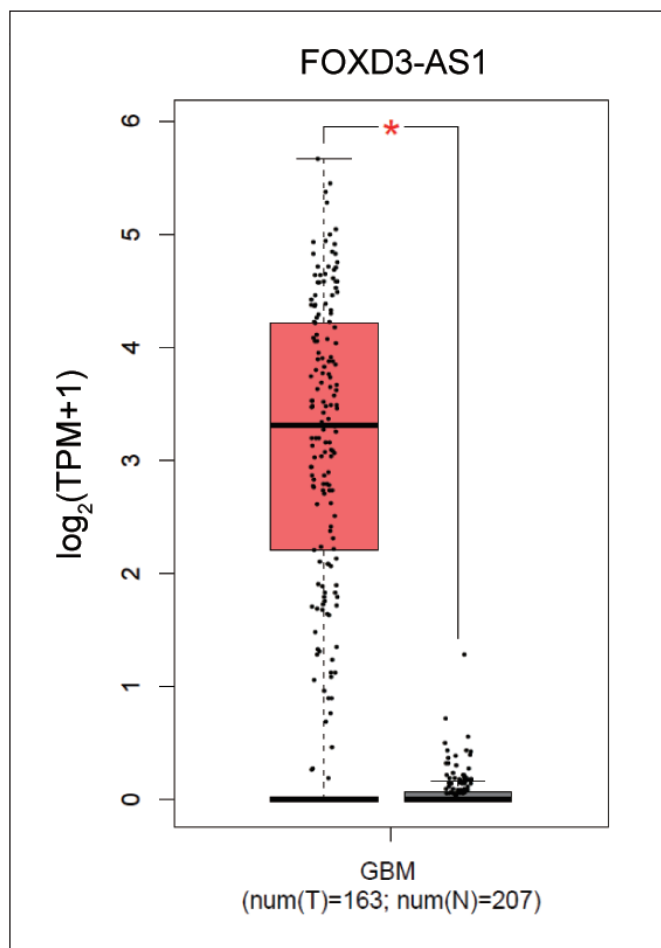
Figure 1: FOXD3-AS1 was upregulated in GBM samples unlike in normal samples, based on the GEPIA database.
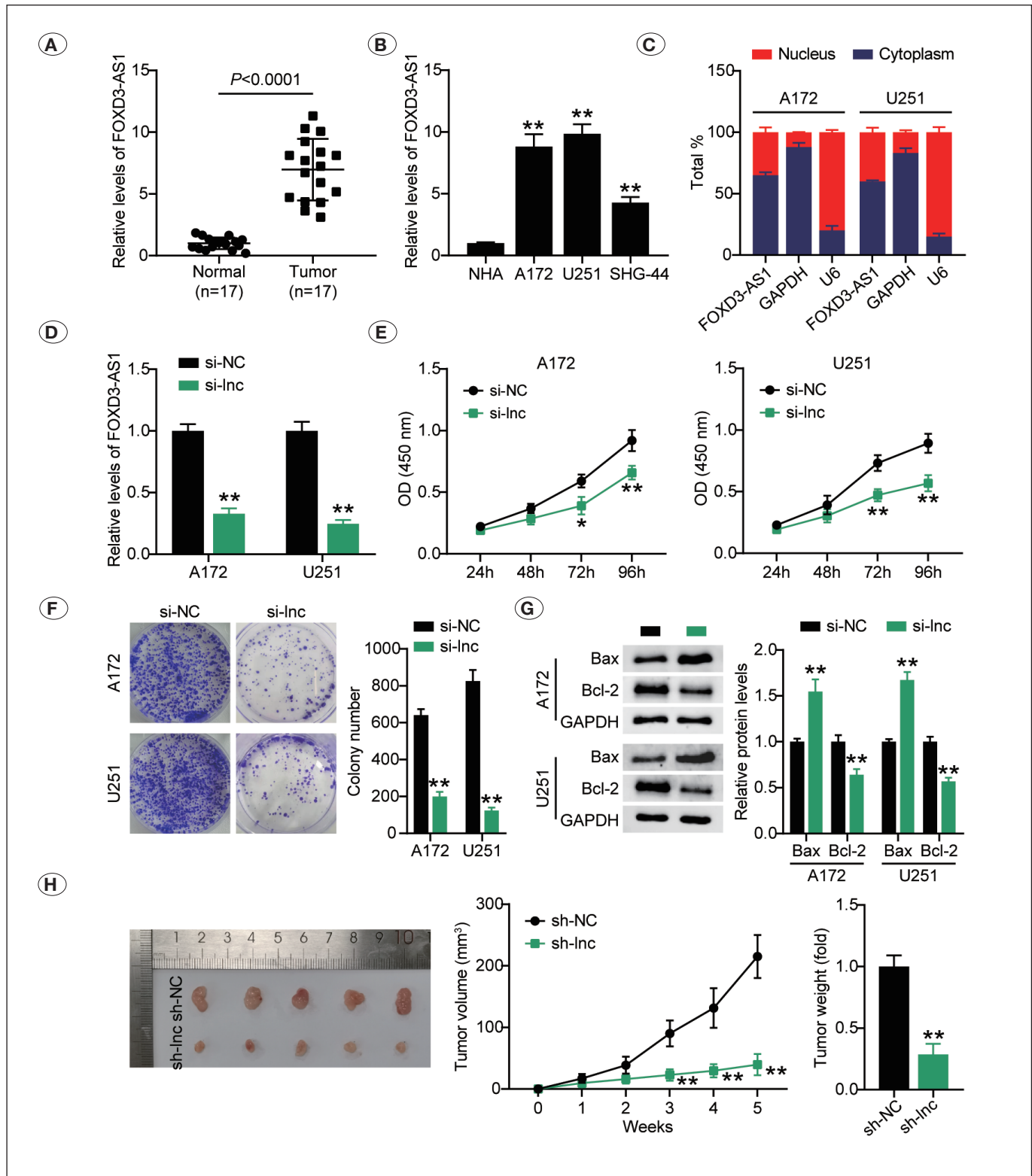
Figure 2: FOXD3-AS1 silencing suppressed glioblastoma growth in vivo and in vitro. **A)** RT-qPCR for FOXD3-AS1 expression in glioblastoma and matched normal brain tissues. **B)** RT-qPCR for FOXD3-AS1 expression in glioblastoma cells and NHA. **C)** The subcellular localization of FOXD3-AS1. **D)** The transfection efficiency of si-FOXD3-AS1 in A172 and U251 cells. **E)** CCK-8 assay for proliferation of transfected A172 and U251cells. **F)** Colony formation assay for colony formation number in transfected A172 and U251cells. **G)** Western blotting for Bcl-2 and Bax levels in transfected A172 and U251 cells. **H)** Tumor growth *in vivo* was identified after C57BL/6 mice injected with FOXD3-AS1 knockdown cells. *p<0.05 and **p<0.001.
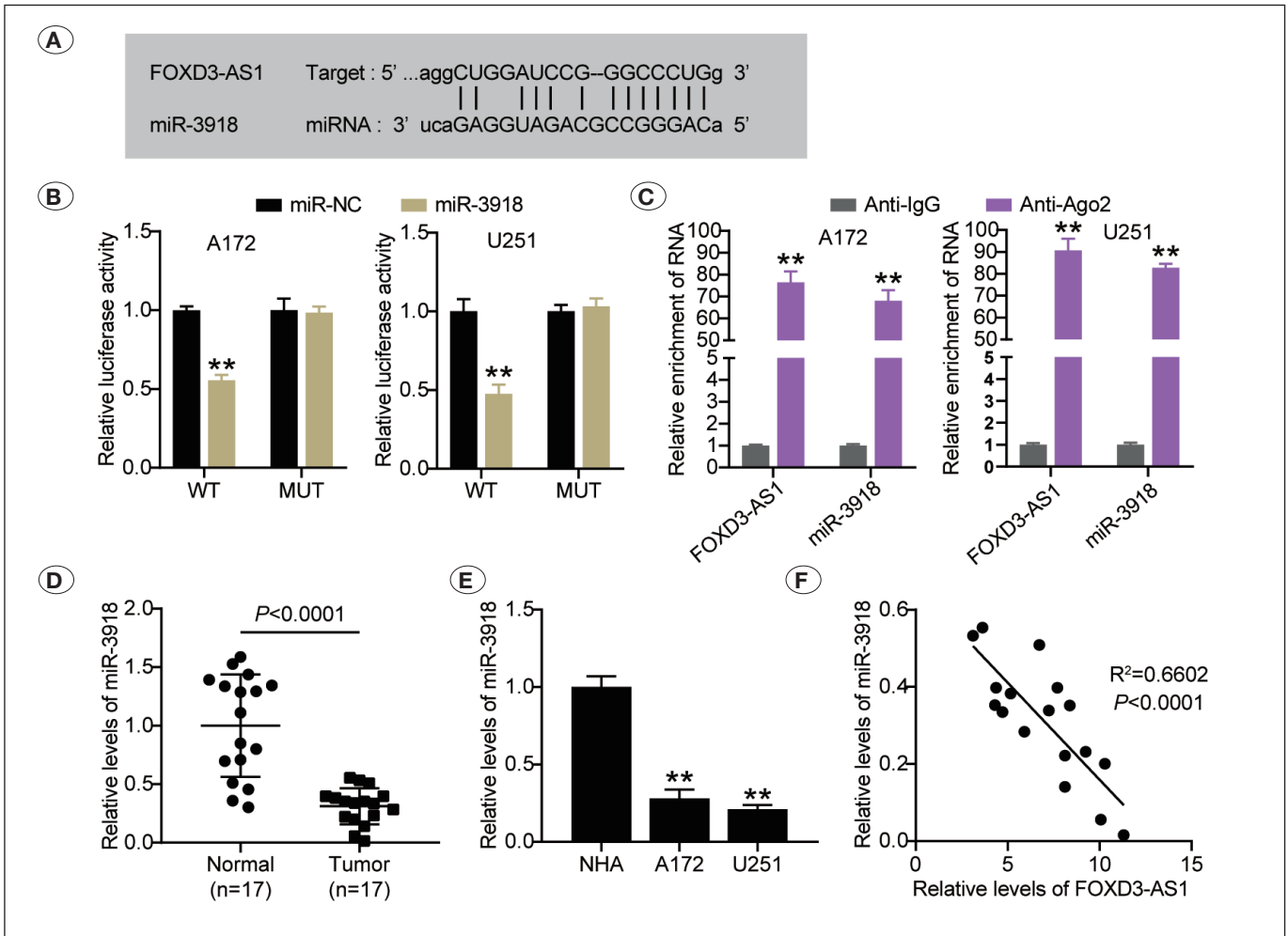
Figure 3: MiR-3918 is targeted by FOXD3-AS1. **A)** TargetScan predicted the binding sites between miR-3918 and FOXD3-AS1. **B)** Luciferase reporter experiment verified the interaction of miR-3918 and FOXD3-AS1. ¨p<0.001 vs. miR-NC. **C)** RIP assay confirmed the binding sites between miR-3918 and FOXD3-AS1. ¨p<0.001 vs. Anti-IgG. **D)** RT-qPCR for miR-3918 expression in glioblastoma and matched normal brain tissues. **E)** RT-qPCR for miR-3918 expression in glioblastoma cells and NHA. ¨p<0.001 vs. NHA. **F)** Pearson's correlation coefficient analyzed the association between miR-3918 and FOXD3-AS1 in glioblastoma tissues.

(Figure 5A). STRING was then applied to determine the key biological processes of the 107 common genes, revealing that WNT5A, EGFR, STAT3, and CCND1 were all related to cell proliferation (Figure 5B). To detect possible interactions with miR-3918, pull-down analysis was conducted with a biotin-labeled-miR-3918 mimic (bio-mimic) or bio-NC. Among the pull-down-candidate-targeted mRNAs, CCND1 mRNA appeared at the top of the list (Figure 5C). Hence, the role of CCND1 in FOXD3-AS1/miR-3918 ceRNA activity has drawn our attention. MiR-3918 binding to 3'UTR-CCND1 mRNA was further confirmed by TargetScan analysis (Figure 5D). Based on the binding fragments, we constructed 3'UTR-CCND1 WT, 3'UTR-CCND1 MUT1, 3'UTR-CCND1 MUT2, and Co-MUT luciferase reporter vectors and introduced them into A172 and U251 cells together with either a miR-3918 mimic or NC. The results of the luciferase reporter assays demonstrated that the miR-3918 mimic contributed to partial or no reduction in luciferase activity mediated by MUT1, MUT2, and Co-MUT.

However, the miR-3918 mimic significantly reduced luciferase activity mediated by 3'UTR-CCND1 WT (Figure 5E). These data suggest that CCND1 is a miR-3918 target. We also measured CCND1 expression in glioblastoma cells and tissue samples. Figures 5F and 5G show the abundant expression of CCND1 detected in clinical tissues and cells. Furthermore, Pearson's analysis revealed that CCND1 levels were negatively correlated with miR-3918 levels in the glioblastoma tissues (Figure 5H). Therefore, the FOXD3-AS1–miR-3918–CCND1 axis was predicted and constructed.

MiR-3918 performs its anti-proliferative function by interacting with CCND1

The effect of miR-3918 recognition on CCND1 was further assessed by transfecting si-CCND1 or miR-3918 inhibitor into A172 and U251 cells. As evidenced by western blotting, the miR-3918 inhibitor rescued the endogenous downregulation of CCND1 in A172 and U251 cells caused by si-CCND1
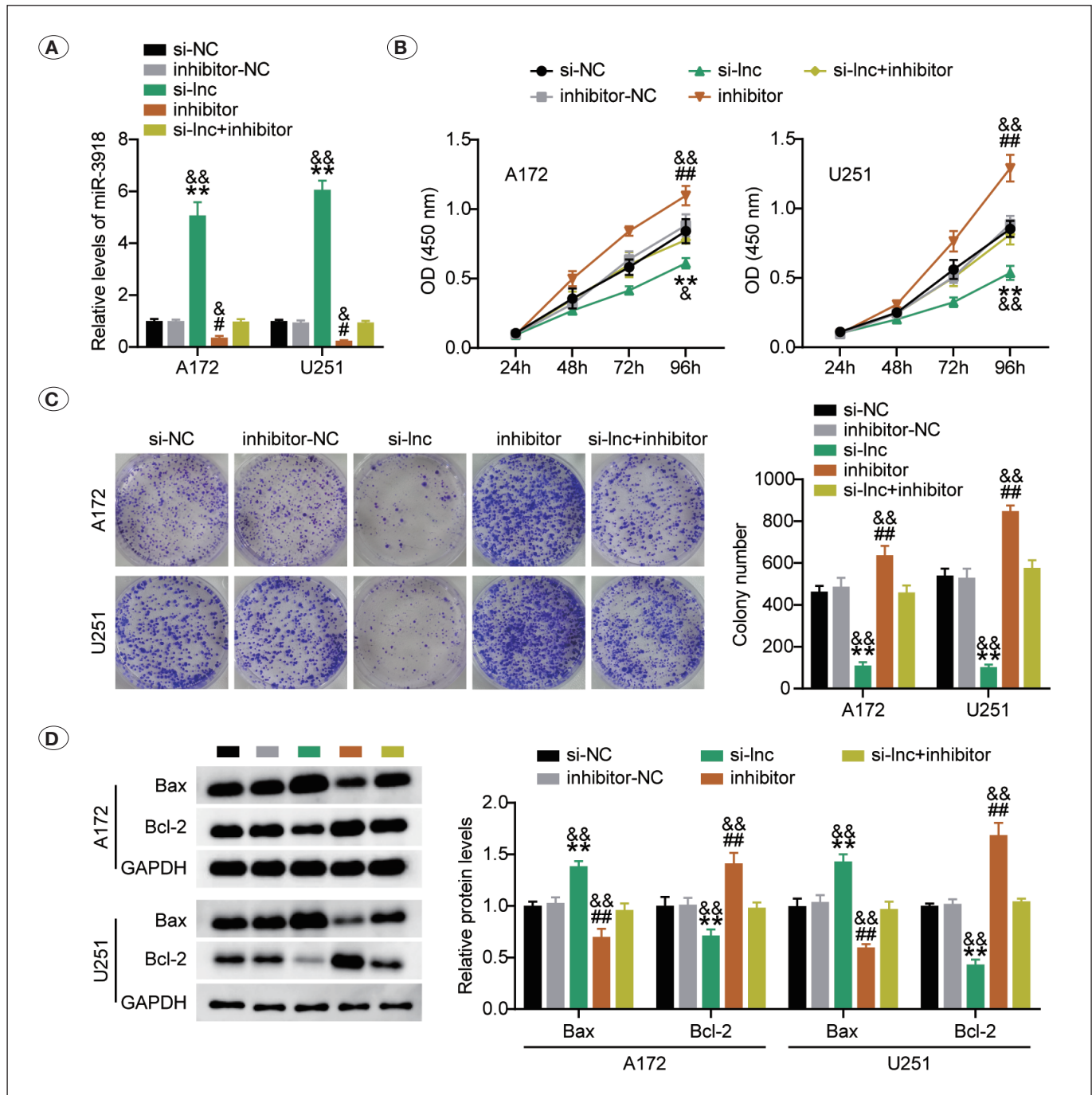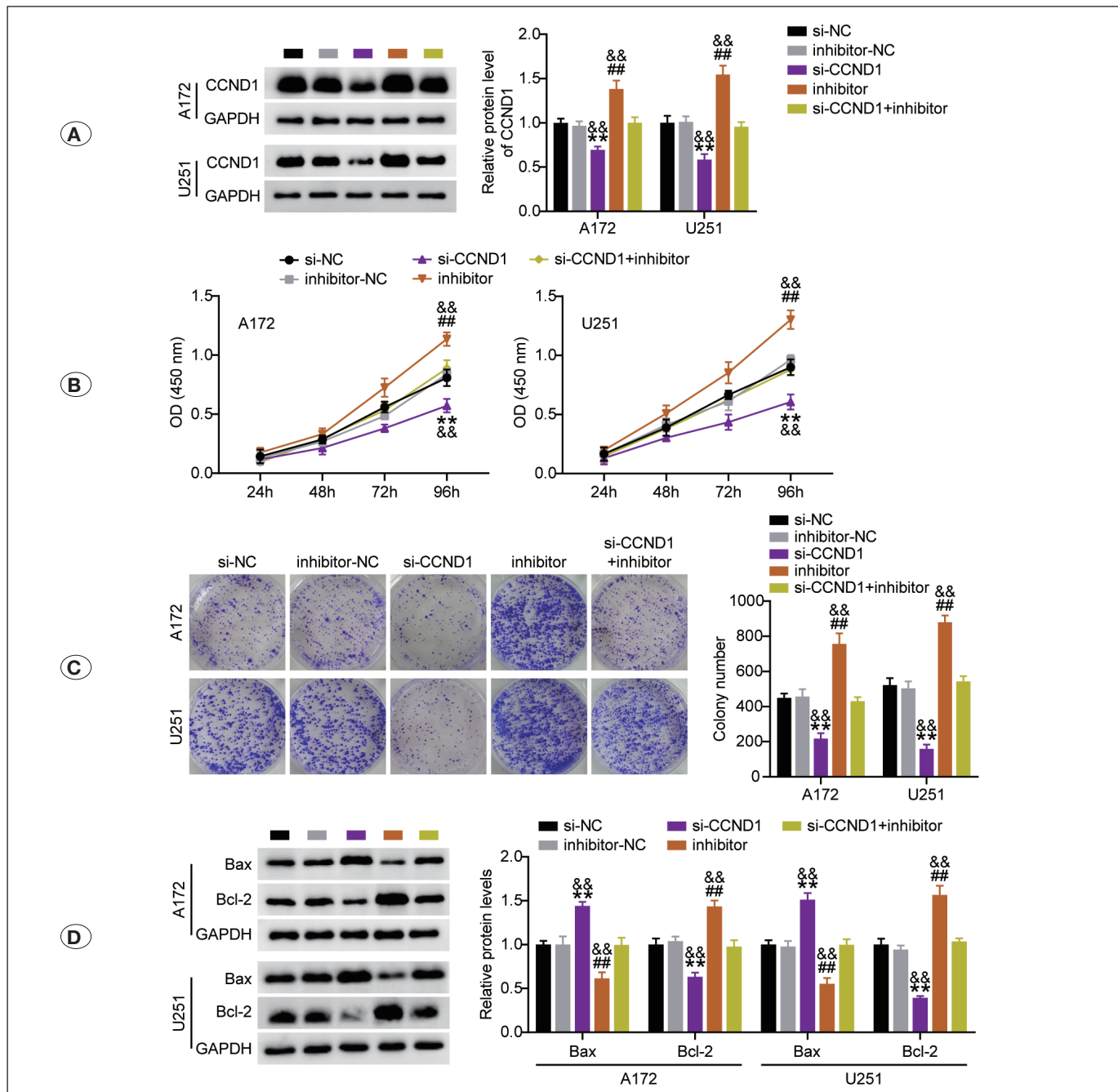
Figure 4: miR-3918 reverses the effect of FOXD3-AS1 on glioblastoma cells. A172 and U251 cells were transfected with si-lncRNA FOXD3-AS1 (si-lnc), si-NC, miR-3918 inhibitor, inhibitor-NC, and si-lnc+inhibitor. **A)** RT-qPCR for miR-3918 expression in transfected cells. **B)** CCK-8 assay for proliferation of transfected cells. **C)** Colony formation assay for colony formation capacity of transfected cells. **D)** Western blotting for Bcl-2 and Bax levels in transfected cells. $^{**}p<0.001$ vs. si-NC; $^{\#}p<0.05$ and $^{\#\#}p<0.001$, inhibitor-NC; $^{\&}p<0.05$ and $^{\&\&}p<0.001$ vs. si-lnc+inhibitor.
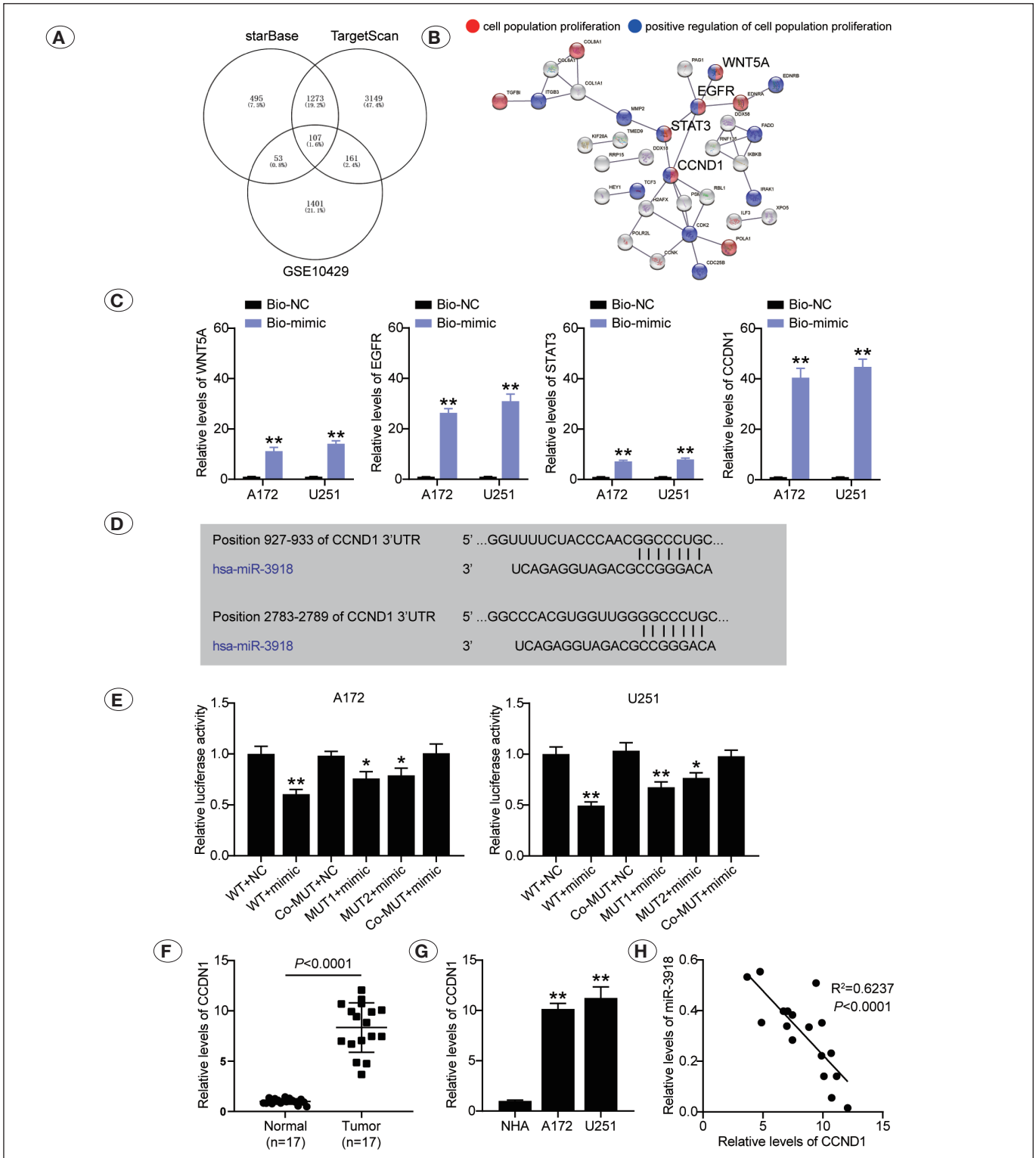
Figure 5: MiR-3918 targets CCND1. **A)** 107 common genes were overlapped from starBase, TargetScan and GSE10429. **B)** STRING identified CCND1, STAT3, EGRF, and WNT5A genes involving cell proliferation. **C)** RNA pull-down assay detected the enrichment of genes in Bio-miR-3918 and Bio-NC groups. $^{**}p<0.001$ vs. Bio-NC. **D)** TargetScan predicted the binding sites between miR-3918 and CCND1. **E)** Luciferase reporter experiment verified the interaction of miR-3918 and CCND1. $^{*}p<0.05$ and $^{**}p<0.001$ vs. miR-NC. **F)** RT-qPCR for CCND1 expression in glioblastoma and matched normal brain tissues. **G)** RT-qPCR for CCND1 expression in glioblastoma cells and NHA. $^{**}p<0.001$ vs. NHA. **H)** Pearson's correlation coefficient analyzed the association between miR-3918 and CCND1 in glioblastoma tissues.

transfection. This suggests that miR-3918 induces CCND1 expression in glioblastoma cells (Figure 6A). CCK-8 experiments demonstrated a reduction in the proliferative capacity among cells with CCND1 silencing. This reduction was rescued by co-transfection with the miR-3918 inhibitor (Figure 6B). Likewise, the loss of CCND1 resulted in a defect in the colony formation capacity of cells, which was recovered by

co-transfection with the miR-3918 inhibitor (Figure 6C). Additionally, the apoptosis triggered by the high Bax and low Bcl-2 expression induced by CCND1 silencing in glioblastoma cells was abrogated by the miR-3918 inhibitor (Figure 6D). Therefore, miR-3918 binds to the CCND1 3'UTR to downregulate its expression, thereby inhibiting the pro-proliferative function of CCND1 in glioblastoma.

Figure 6: CCND1 recovers the effect of miR-3918 on glioblastoma cells. A172 and U251 cells were transfected with si-CCND1, si-NC, inhibitor, inhibitor-NC and si-CCND1+inhibitor. **A)** Western blotting for CCND1 expression in transfected cells. **B)** CCK-8 assay for cell proliferation in transfected cells. **C)** Colony formation assay for colony formation capacity of transfected cells. **D)** Western blotting for Bcl-2 and Bax levels in transfected cells. $^{**}p<0.001$ vs. si-NC; $^{\#\#}p<0.001$ vs. inhibitor-NC; $^{\&\&}p<0.001$ vs. si-CCND1+inhibitor.

■ DISCUSSION

In the present study, we observed that FOXD3-AS1 is highly expressed in glioblastoma cells and tissues. *In vivo* and *in vitro* functional research indicated that the downregulation of FOXD3-AS1 not only constrained glioblastoma cell growth *in vitro* but also suppressed glioblastoma tumorigenesis *in vivo*. Mechanistically, FOXD3-AS1 functioned as an oncogenic propellant by regulating the miR-3918/CCND1 axis. Therefore, we first demonstrated that FOXD3-AS1 competitively sequesters miR-3918, thereby upregulating CCND1 expression and facilitating CCND1 oncogenicity during glioblastoma malignancy. These findings suggest a novel target for glioblastoma intervention.

We observed higher levels of FOXD3-AS1 in glioblastoma tissues and cells than in NHAs and normal brain tissues, suggesting its potential role in tumorigenesis. Our results are also congruent with those that demonstrated high FOXD3-AS1 expression in several cancers, such as cutaneous malignant melanoma (4), nasopharyngeal carcinoma (23), and lung cancer (8). Previous studies have unambiguously demonstrated the pro-oncogenic functions of FOXD3-AS1 in several malignancies. For instance, FOXD3-AS1 silencing curbs hepatocellular carcinoma by deactivating the AKT pathway (10). Loss of FOXD3-AS1 exerts its anti-tumor action in thyroid cancer via the TGF-β1/Smad signaling pathway (5). *In vitro* and *in vivo* studies have also demonstrated the inhibitory influence of FOXD3-AS1 silencing on colon adenocarcinoma growth (25). Despite these, FOXD3-AS1's role in glioblastoma remains to be elucidated. We used shRNA interference to silence FOXD3-AS1 expression in A172 and U251 cells. Subsequent cellular function assays demonstrated that FOXD3-AS1 knockdown diminished the proliferative capacity of glioblastoma cells and accelerated their apoptosis. Next, subcutaneously transplanted tumor models were used to validate FOXD3-AS1 function *in vivo*. It is not surprising that FOXD3-AS1 silencing led to slower tumor growth. Therefore, FOXD3-AS1 may function as an oncogenic lncRNA to promote glioblastoma malignancy.

lncRNAs interact with proteins, miRNAs, and mRNAs, and exert coding-independent functions in glioblastoma genesis and progression (3). Among the mechanisms of action of lncRNAs, ceRNA activity in cancer has been extensively studied. Thus, lncRNAs can titrate miRNAs and inhibit their activity via target binding (16). To explore the regulatory mechanism of FOXD3-AS1, we analyzed its nuclear and cytoplasmic distribution in glioblastoma cells. Our findings revealed that FOXD3-AS1 is predominantly located in the cytoplasm, suggesting its ceRNA activity for miRNAs. According to our bioinformatic prediction, FOXD3-AS1 physically binds to miR-3918. To date, the tumor-suppressive role of miR-3918 has been demonstrated in gastric cancer (6), and hepatocellular carcinoma (20). For example, miR-3918 inactivates the oncogenic activity of NF-κB-dependent malignancy in hepatocellular carcinoma via its target (Bcl-2) (6). MiR-3918 could also function as a tumor suppressor and abrogate the strengthened malignant behavior of gastric cancer cells (6). However, its biofunction in glioblastoma remains to be clarified. We observed that miR-3918 was downregulated in glioblastoma cells and tissues.

The results of our cell functional assays demonstrated that the reduction in miR-3918 endogenous expression can strengthen the proliferative capacity and attenuate apoptosis in glioblastoma cells. In line with earlier studies (6,20), miR-3918 may act as an anti-oncomir in glioblastoma. The competitive interaction between miR-3918 and FOXD3-AS1 was also illustrated through luciferase reporter and RIP assays. These interactions were further supported by the negative correlation between their expression in clinical samples. More importantly, the miR-3918 inhibitor rescued the proliferative defect in glioblastoma cells resulting from FOXD3-AS1 silencing. Our findings reveal a novel mechanism for FOXD3-AS1 ceRNA activity during glioblastoma malignancy.

Competitive miRNA-mRNA binding is a critical step in lncRNA-mediated ceRNA activity (22). As indicated by our bioinformatics analysis, we discovered that WNT5A, EGFR, STAT3, and CCND1 are potential targets of miR-3918 in glioblastoma. Among them, CCND1 was of interest because it had the highest enrichment in the biotin-labeled miR-3918 pull-down assay. CCND1 is located on chromosome 11q13.3, and consists of five exons. It encodes one of the proteins in the highly conserved cyclin family, which is characterized by dramatic periodicity in protein abundance during the cell cycle. Its dysregulation can alter cell cycle progression and is frequently observed in a variety of cancers such as gastric (14), breast (11), and lung (21). In glioblastoma, CCND1 has been recognized as an oncoprotein (17). For example, CCND1 degradation induced by deubiquitination has an anti-glioblastoma effect (17). Conversely, enforced CCND1 expression facilitates glioblastoma dissemination (2). Consistently, we also observed amplification of CCND1 in glioblastoma tissues and cells. Furthermore, silencing of CCND1 attenuated cellular proliferation and triggered apoptosis in glioblastoma cells. These results underpin the oncogenic role of CCND1 in glioblastoma progression. Next, we explored the upstream regulation in glioblastoma. We validated that CCND1 is a miR-3918 target in glioblastoma cells. This competitive interaction was further evidenced by the inverse relationship between their expression levels in clinical samples. Additionally, miR-3918 inhibition resulted in an evident increase in CCND1 levels. Interestingly, silencing of CCND1 abrogated the uncontrolled proliferation of glioblastoma cells caused by the miR-3918 inhibitor. Therefore, miR-3918 targets CCND1 and inhibits its pro-proliferative effect on glioblastoma cells, resulting in glioblastoma suppression.

Notably, the regulatory mechanisms of lncRNAs are complex as each lncRNA or miRNA can bind to different target genes. Therefore, future investigations of their interactions may enrich our understanding of the mechanism of FOXD3-AS1 in glioblastoma. Furthermore, more clinical samples are required to verify the differential expression of these genes.

■ CONCLUSION

Our data demonstrate the FOXD3-AS1's oncogenic role during glioblastoma progression. Silencing FOXD3-AS1 weakens proliferation and promotes apoptosis of glioblastoma cells. Mechanical investigations have revealed the oncogenic ef-

fects of FOXD3-AS1 in glioblastoma, at least partially, through the miR-3918/CCND1 axis, providing a novel therapeutic approach for glioblastoma.

■ REFERENCES

1. Bhan A, Soleimani M, Mandal SS: Long noncoding RNA and cancer: A new paradigm. Cancer Res 77:3965-3981, 2017

2. Cemeli T, Guasch-Vallés M, Nàger M, Felip I, Cambray S, Santacana M, Gatius S, Pedraza N, Dolcet X, Ferrezuelo F, Schuhmacher AJ, Herreros J, Garí E: Cytoplasmic cyclin D1 regulates glioblastoma dissemination. J Pathol 248:501-513, 2019

3. Chan JJ, Tay Y: Noncoding RNA: RNA regulatory networks in cancer. Int J Mol Sci 19:1310, 2018

4. Chen X, Gao J, Yu Y, Zhao Z, Pan Y: LncRNA FOXD3-AS1 promotes proliferation, invasion and migration of cutaneous malignant melanoma via regulating miR-325/MAP3K2. Biomed Pharmacother 120:109438, 2019

5. Chen Y, Gao H, Li Y: Inhibition of LncRNA FOXD3-AS1 suppresses the aggressive biological behaviors of thyroid cancer via elevating miR-296-5p and inactivating TGF-β1/Smads signaling pathway. Mol Cell Endocrinol 500:110634, 2020

6. Fu T, Ji K, Jin L, Zhang J, Wu X, Ji X, Fan B, Jia Z, Wang A, Liu J, Bu Z, Ji J: ASB16-AS1 up-regulated and phosphorylated TRIM37 to activate NF-κB pathway and promote proliferation, stemness, and cisplatin resistance of gastric cancer. Gastric Cancer 24:45-59, 2021

7. Gimple RC, Bhargava S, Dixit D, Rich JN: Glioblastoma stem cells: Lessons from the tumor hierarchy in a lethal cancer. Genes Dev 33:591-609, 2019

8. Ji T, Zhang Y, Wang Z, Hou Z, Gao X, Zhang X: FOXD3-AS1 suppresses the progression of non-small cell lung cancer by regulating miR-150/SRCIN1axis. Cancer Biomark 29:417-427, 2020

9. Le Rhun E, Preusser M, Roth P, Reardon DA, van den Bent M, Wen P, Reifenberger G, Weller M: Molecular targeted therapy of glioblastoma. Cancer Treat Rev 80:101896, 2019

10. Liu C, Zhang M, Zhao J, Zhu X, Zhu L, Yan M, Zhang X, Zhang R: LncRNA FOXD3-AS1 mediates AKT pathway to promote growth and invasion in hepatocellular carcinoma through regulating RICTOR. Cancer Biother Radiopharm 35:292-300, 2020

11. Liu X, Yao W, Xiong H, Li Q, Li Y: LncRNA NEAT1 accelerates breast cancer progression through regulating miR-410-3p/CCND1 axis. Cancer Biomark 29:277-290, 2020

12. Livak KJ, Schmittgen TD: Analysis of relative gene expression data using real-time quantitative PCR and the 2(-Delta Delta C(T)) Method. Methods 25:402-408, 2001

13. Lu C, Wei Y, Wang X, Zhang Z, Yin J, Li W, Chen L, Lyu X, Shi Z, Yan W, You Y: DNA-methylation-mediated activating of lncRNA SNHG12 promotes temozolomide resistance in glioblastoma. Mol Cancer 19:28, 2020

14. Nie M, Wang Y, Yu Z, Li X, Deng Y, Wang Y, Yang D, Li Q, Zeng X, Ju J, Liu M, Zhao Q: AURKB promotes gastric cancer progression via activation of CCND1 expression. Aging 12:1304-1321, 2020

15. Peng WX, Koirala P, Mo YY: LncRNA-mediated regulation of cell signaling in cancer. Oncogene 36:5661-5667, 2017

16. Qi M, Yu B, Yu H, Li F: Integrated analysis of a ceRNA network reveals potential prognostic lncRNAs in gastric cancer. Cancer Med 9:1798-1817, 2020

17. Sun T, Xu YJ, Jiang SY, Xu Z, Cao BY, Sethi G, Zeng YY, Kong Y, Mao XL: Suppression of the USP10/CCND1 axis induces glioblastoma cell apoptosis. Acta Pharmacol Sin 42:1338-1346, 2021

18. Voce DJ, Bernal GM, Wu L, Crawley CD, Zhang W, Mansour NM, Cahill KE, Szymura SJ, Uppal A, Raleigh DR, Spretz R, Nunez L, Larsen G, Khodarev NN, Weichselbaum RR, Yamini B: Temozolomide treatment induces lncRNA MALAT1 in an NF-κB and p53 codependent manner in glioblastoma. Cancer Res 79:2536-2548, 2019

19. Wirsching HG, Galanis E, Weller M: Glioblastoma. Handb Clin Neurol 134:381-397, 2016

20. Yang G, Wang X, Liu B, Lu Z, Xu Z, Xiu P, Liu Z, Li J: Circ-BIRC6, a circular RNA, promotes hepatocellular carcinoma progression by targeting the miR-3918/Bcl2 axis. Cell Cycle 18:976-989, 2019

21. Yang Y, Lu T, Li Z, Lu S: FGFR1 regulates proliferation and metastasis by targeting CCND1 in FGFR1 amplified lung cancer. Cell Adh Migr 14:82-95, 2020

22. Yao Y, Zhang T, Qi L, Zhou C, Wei J, Feng F, Liu R, Sun C: Integrated analysis of co-expression and ceRNA network identifies five lncRNAs as prognostic markers for breast cancer. J Cell Mol Med 23:8410-8419, 2019

23. Zhang E, Li C, Xiang Y: LncRNA FOXD3-AS1/miR-135a-5p function in nasopharyngeal carcinoma cells. Open Med 15:1193-1201, 2020

24. Zhou M, Zhang Z, Zhao H, Bao S, Cheng L, Sun J: An immune-related six-lncRNA signature to improve prognosis prediction of glioblastoma multiforme. Mol Neurobiol 55:3684-3697, 2018

25. Zhu FY, Zhang SR, Wang LH, Wu WD, Zhao H: LINC00511 promotes the progression of non-small cell lung cancer through downregulating LATS2 and KLF2 by binding to EZH2 and LSD1. Eur Rev Med Pharmacol Sci 23:8377-8390, 2019